Supporting Information

Dissociative Water Adsorption by $Al_3O_4^+$ in the Gas Phase

Matias R. Fagiani,[1,2], Xiaowei Song,[1,2] Sreekanta Debnath,[1,2] Sandy Gewinner,[2] Wieland Schöllkopf,[2] Knut R. Asmis,[1,*] Florian A. Bischoff,[3] Fabian Müller,[3] and Joachim Sauer [3,*]

[1]*Wilhelm-Ostwald-Institut für Physikalische und Theoretische Chemie, Universität Leipzig, Linnéstrasse 2, D-04103 Leipzig, Germany*

[2]*Fritz-Haber-Institut der Max-Planck-Gesellschaft, Faradayweg 4-6, D-14195 Berlin, Germany*

[3]*Institut für Chemie, Humboldt-Universität zu Berlin, Unter den Linden 6, D-10099 Berlin, Germany*

S1. Additional experimental details

A pulsed beam of cationic aluminum-oxide clusters is formed by laser vaporization using a rotating rod source. Vaporization is induced by focusing the second harmonic output (532 nm, ~4 mJ) of a pulsed 50 Hz Nd:YAG laser (Quantel, Q-smart 100) onto the surface of a moving aluminum-rod target. The ablated atoms and ions are entrained in a carrier gas pulse of 0.16 % O_2 seeded in helium, which is expanded through a clustering channel into vacuum. The source has been recently modified to allow the use of a second pulsed valve. A flow of helium (1.5 bar) passes through a bubbler containing D_2O, enters the source block through a second gas channel and meets the clustering channel 8 mm before the nozzle. $Al_mO_o^+(D_2O)_n$ complexes with $n \leq$ 6-8 are efficiently formed (see Figure S1).

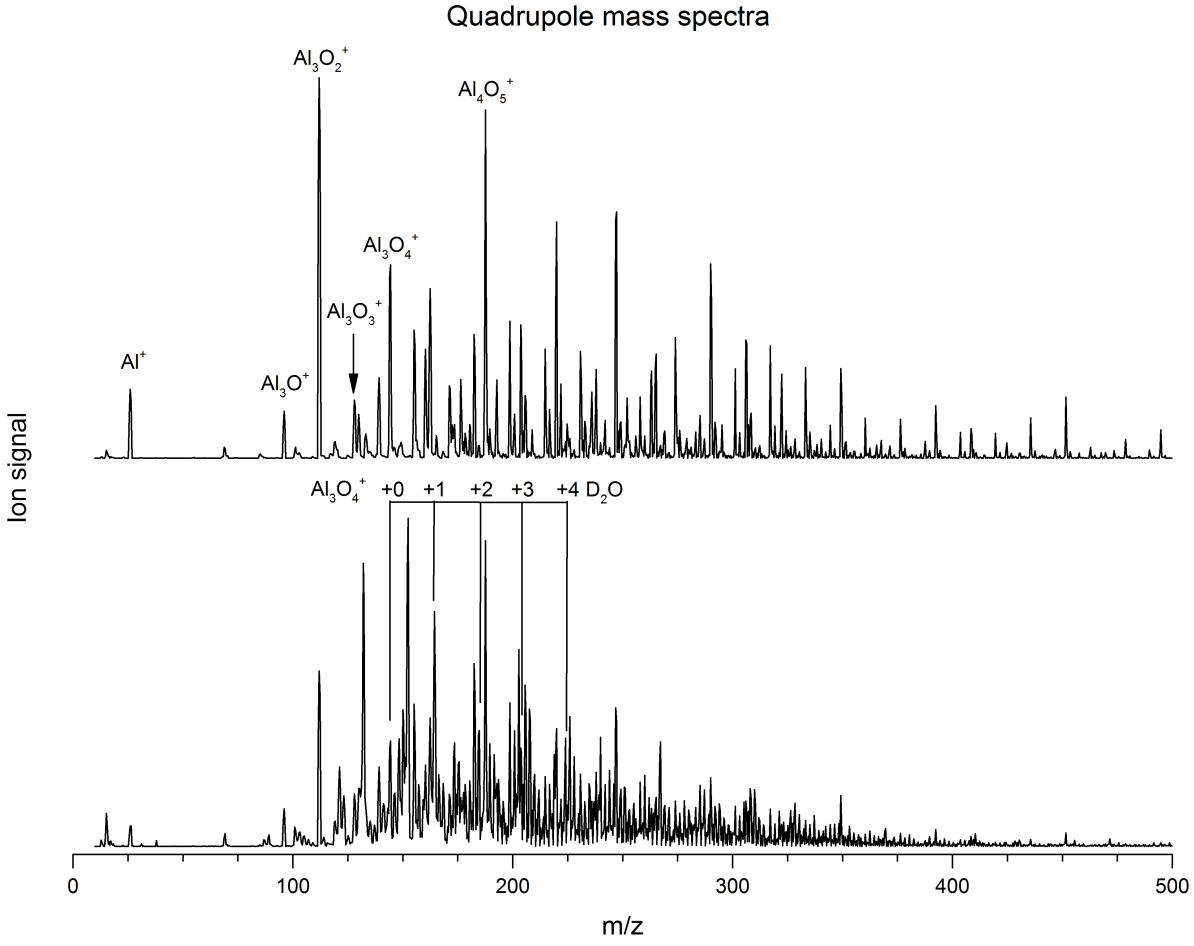

Figure S1 Quadrupole mass spectra of aluminum oxide cations produced by laser vaporization source without (top) and with D_2O (bottom) added to the second gas channel.

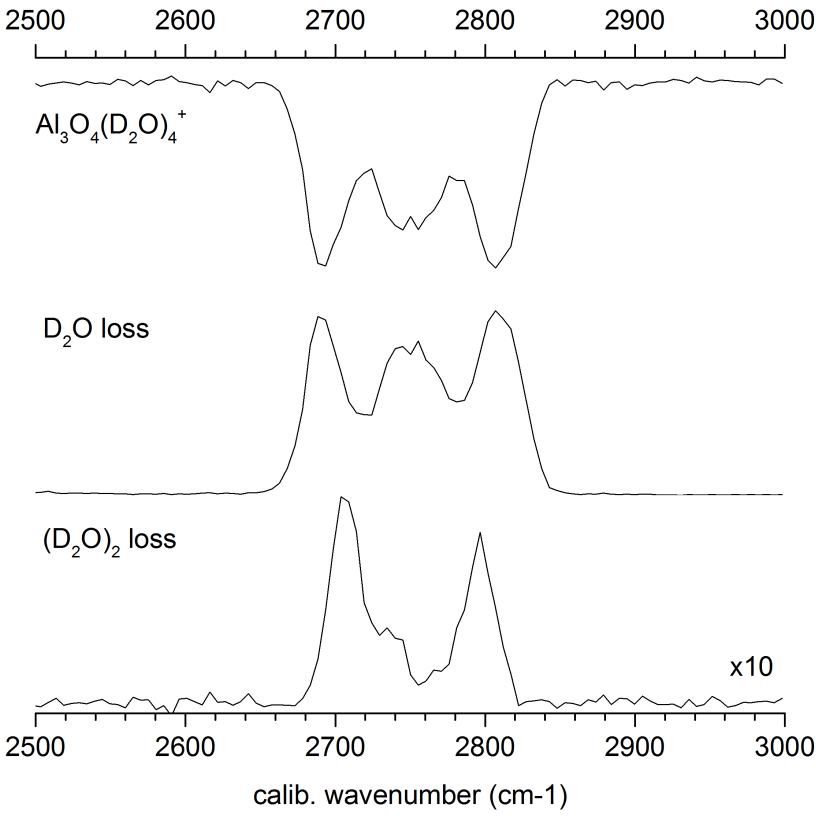

Figure S2 Ion yield spectra for IRMPD of $[Al_3O_4(D_2O)_4]^+$ from 2500 to 3000 cm^{-1} obtained with the FHI-FEL. The depletion of parent ion (top trace) and the formation of the two most abundant fragment ions (lower traces) are shown. Under these conditions, loss of a single D_2O molecule is the dominant fragmentation channel and ten times more efficient then loss of two D_2O molecules.

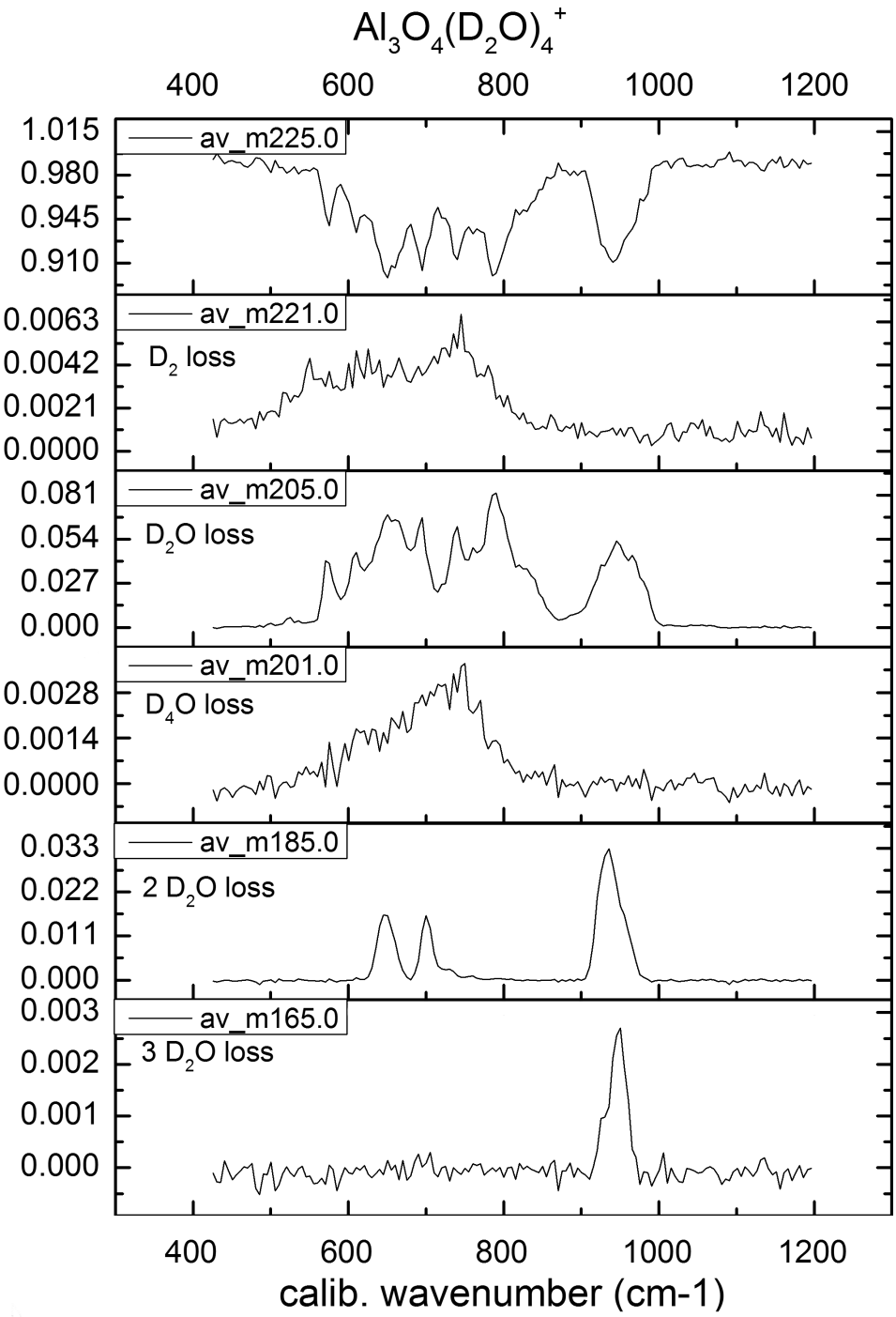

Figure S3 Ion yield spectra for IRMPD of $[Al_3O_4(D_2O)_4]^+$ from 410 to 1200 cm^{-1} obtained with the FHI-FEL. The depletion of parent ion (top trace) and the formation of the five most abundant fragment ions (lower traces) are shown. Under these conditions, loss of a single D_2O molecule is the dominant fragmentation channel.

S2. Experimental spectra compared to computed spectra for different isomers

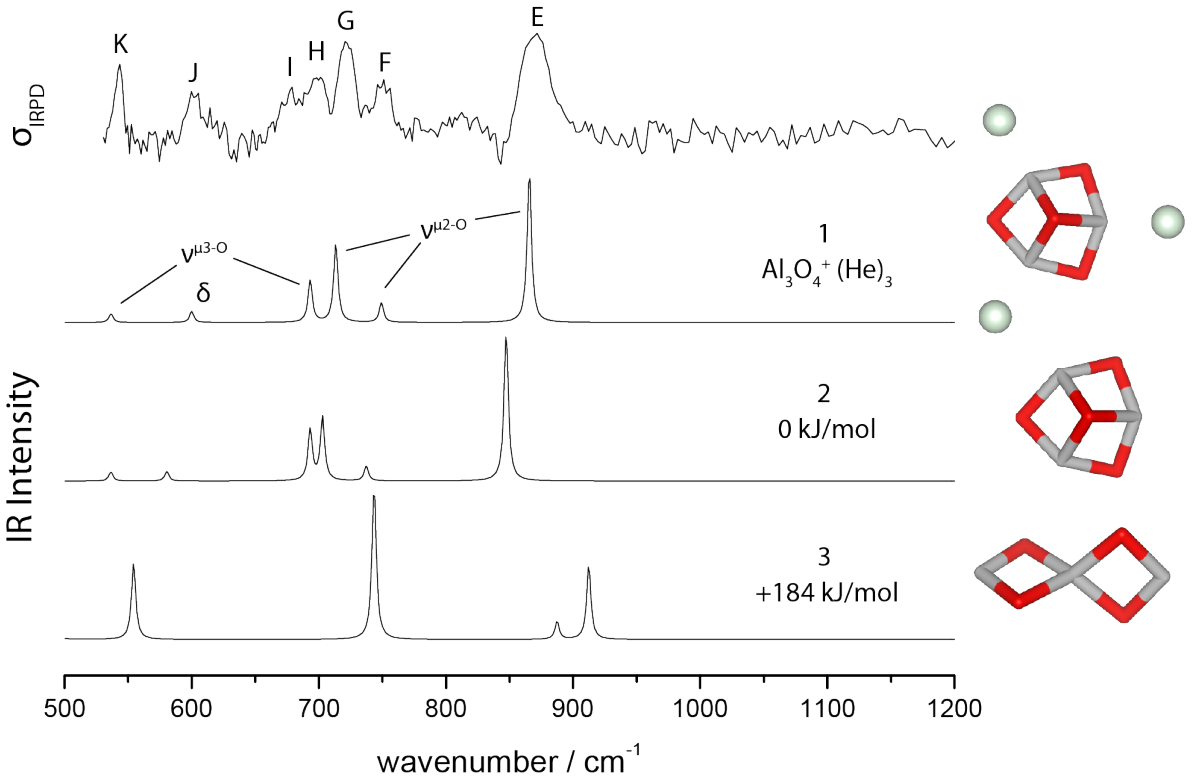

Figure S4 IRPD vibrational spectrum (top) of $Al_3O_4^+ \cdot (He)_{1-3}$ compared with B3LYP/TZVPP harmonic frequencies and intensities of low lying structures with and without He-tag and convoluted with a Gaussian line shape function (fwhm width: 10 cm^{-1}). See Table S1 for band assignments. The relative energy including vibrational zero point energy of each isomer is given in kJ/mol.

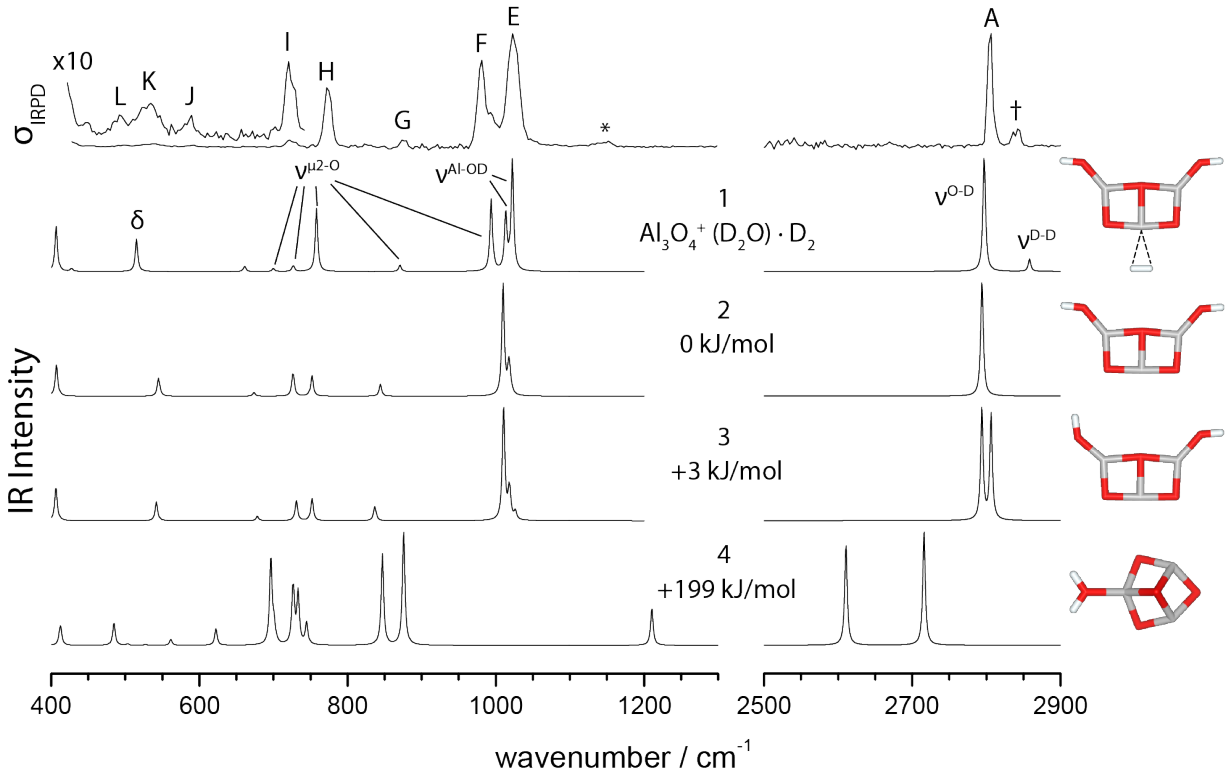

Figure S5 IRPD vibrational spectrum (top) of $[Al_3O_4\ (D_2O)]^+ \cdot D_2$ compared with B3LYP/ TZVPP harmonic frequencies (scaled with the factor 0.9732 above 2000 cm^{-1}) and intensities of low lying structures with and without D_2-tag and convoluted with a Gaussian line shape function (fwhm width: 10 cm^{-1}). See Table S1 for band assignments. The relative energy including vibrational zero point energy of each isomer is given in kJ/mol.

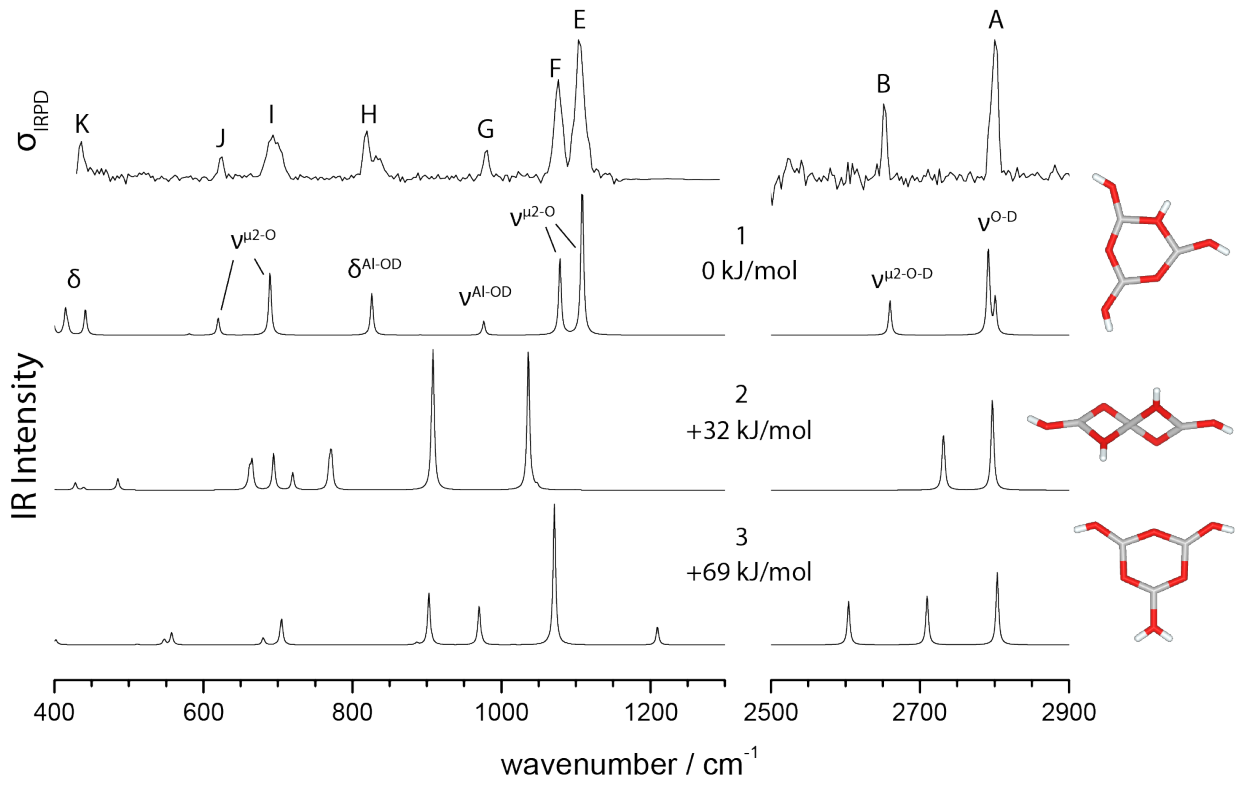

Figure S6 IRPD vibrational spectrum (top) of $[Al_3O_4\ (D_2O)_2]^+ \cdot D_2$ compared with B3LYP/ TZVPP harmonic frequencies (scaled with the factor 0.9732 above 2000 cm^{-1}) and intensities of low lying structures convoluted with a Gaussian line shape function (fwhm width: 10 cm^{-1}). See Table S1 for band assignments. The relative energy including vibrational zero point energy of each isomer is given in kJ/mol.

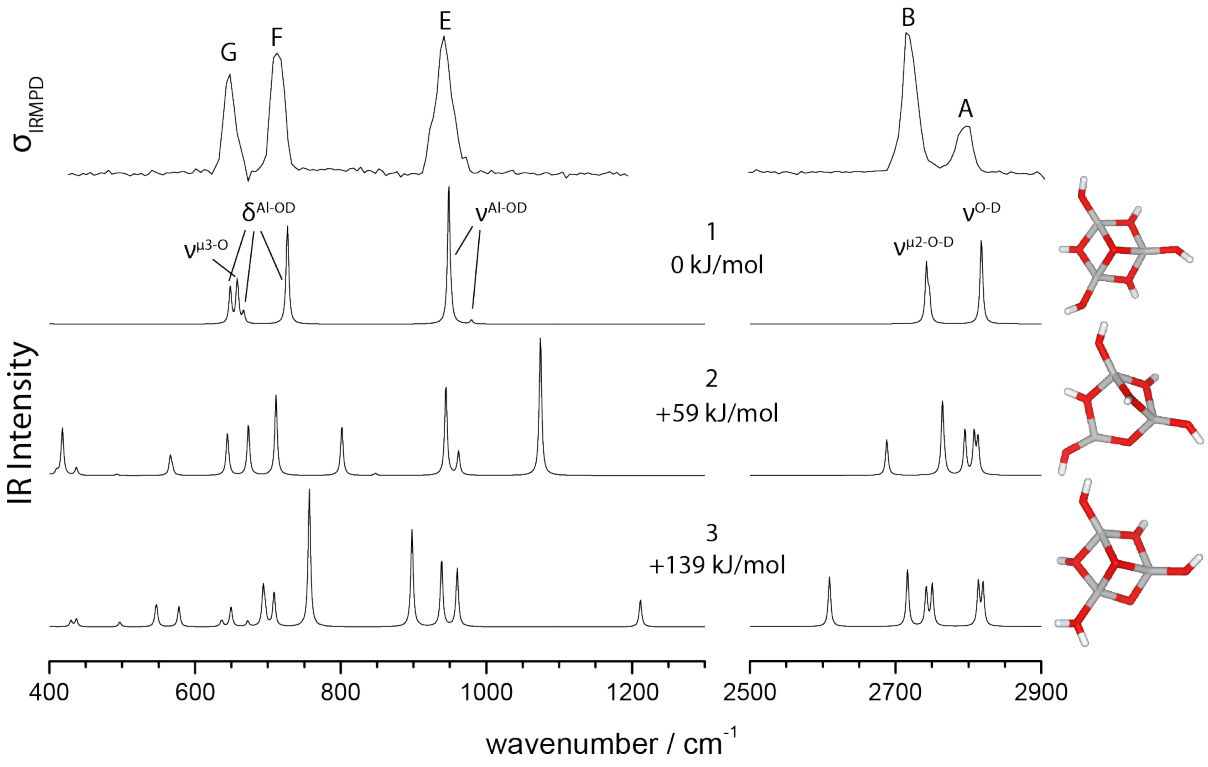

Figure S7 IRMPD vibrational spectrum (top) of $[Al_3O_4\ (D_2O)_3]^+$ compared with B3LYP/ TZVPP harmonic frequencies (scaled with the factor 0.9732 above 2000 cm^{-1}) and intensities of low lying structures convoluted with a Gaussian line shape function (fwhm width: 10 cm^{-1}). See Table S1 for band assignments. The relative energy including vibrational zero point energy of each isomer is given in kJ/mol.

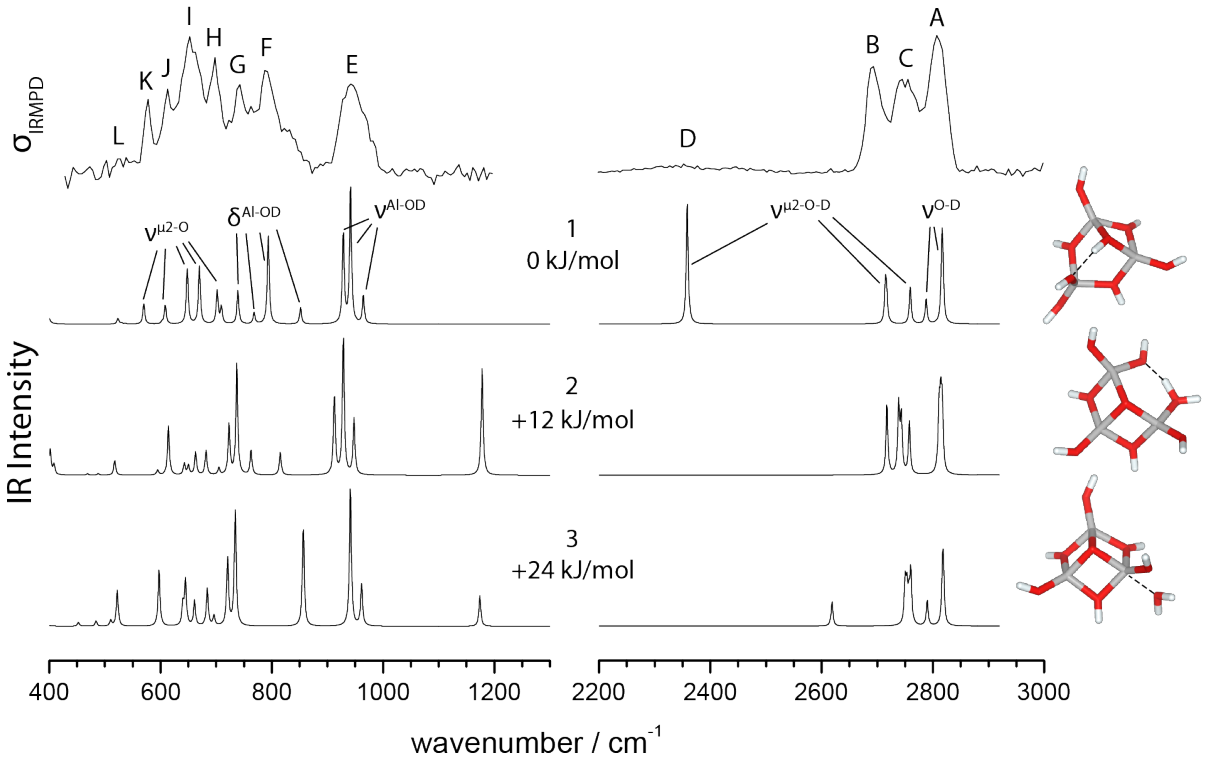

Figure S8 IRMPD vibrational spectrum (top) of $[Al_3O_4\ (D_2O)_4]^+$ compared with B3LYP/ TZVPP harmonic frequencies (scaled with the factor 0.9732 above 2000 cm^{-1}) and intensities of low lying structures convoluted with a Gaussian line shape function (fwhm width: 10 cm^{-1}). See Table S1 for band assignments. The relative energy including vibrational zero point energy of each isomer is given in kJ/mol.

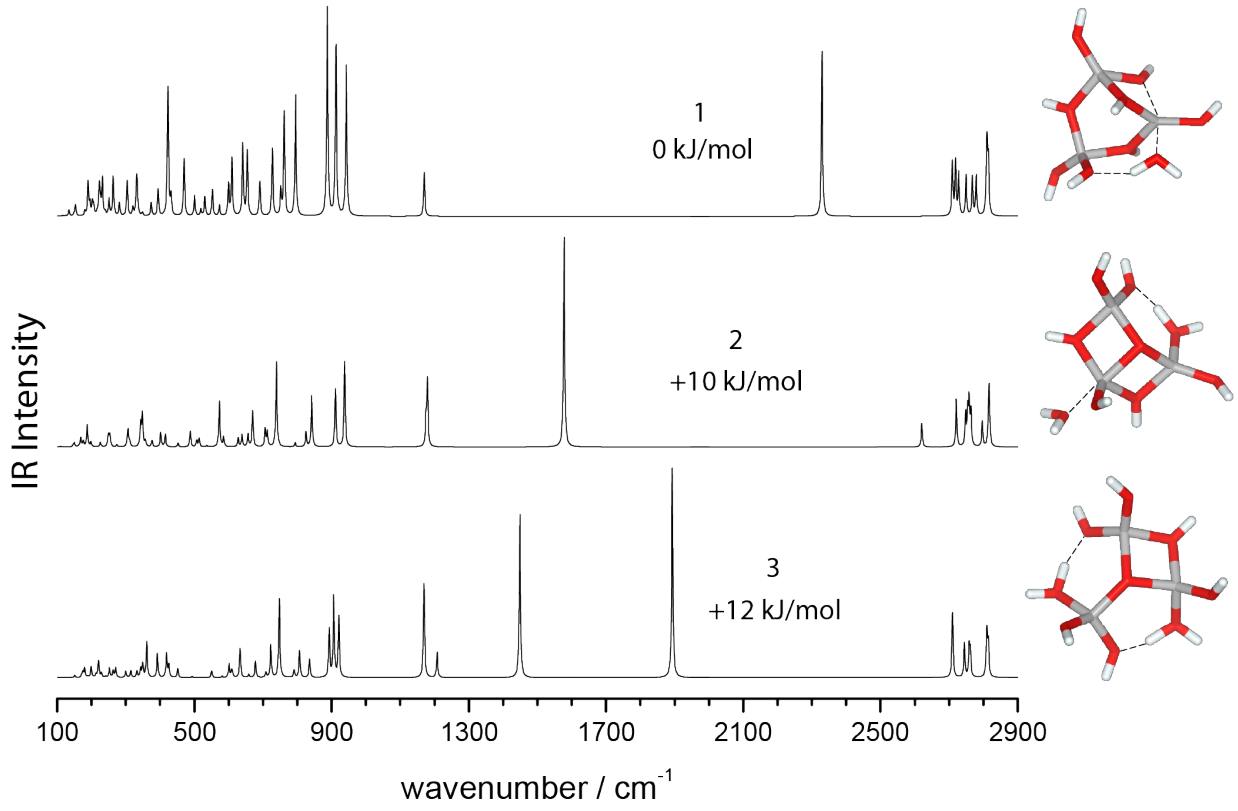

Figure S9 B3LYP/TZVPP harmonic frequencies (scaled with the factor 0.9732 above 2000 cm^{-1}) and intensities of low lying structures of $[Al_3O_4 (D_2O)_5]^+$ convoluted with a Gaussian line shape function (fwhm width: 10 cm^{-1}). See Table S1 for band assignments. The relative energy including vibrational zero point energy of each isomer is given in kJ/mol.

S3. Experimental and calculated vibrational wavenumbers

Table S1 Experimental IRPD/IRMPD band positions (in cm^{-1}), B3LYP/TZVPP harmonic frequencies (in cm^{-1}) of the lowest energy isomer and normal mode assignments for $[Al_3O_4(D_2O)_n]^+$ with $n = 0 – 4$. Frequencies above 2000 cm^{-1} were scaled with 0.9732.

System	Exp	DFT (scaled above 2000 cm^{-1})	Assignment
***n* = 0**[a]	871 (E), 750 (F), 722 (G), 700 (H)	866, 865, 752, 749, 713, 713	Al_2-(μ_2-O) stretch
	678 (I), 543 (K)	693, 537, 536	Al_3-(μ_3-O) stretch
	602 (J)	600	frame deformation (μ_3-O)
***n* = 1**[b]	2842 (†)	2858	D-D stretch
	2806 (A)	2798, 2797	terminal Al-(O-D) stretch
	1023 (E)	1022, 1014	Al-OD stretch
	971 (F), 873 (G), 772 (H), 722 (I)	994, 871[c] ,758 ,727, 700	Al_2-(μ_2-O) and Al_3-(μ_3-O) stretch
	593 (J), 539 (K), 497 (L)	515	frame deformation (μ_3-O)
***n* = 2**	2800 (A)	2801, 2793, 2791	terminal Al-(O-D) stretch
	2651 (B)	2659	bridging Al_2-(μ_2-O-D) stretch
	1104 (E), 1077 (F)	1109, 1079	Al_2-(μ_2-O) stretch
	981 (G)	976, 891, 857	Al-OD stretch
	694 (I), 625 (J)	689, 620	Al_2-(μ_2-O) stretch
	819 (H)	826	Al_2-(μ_2-OD) in-plane bend
	436 (K)	442	Al_2-(μ_2-OD) out-of-plane bend
***n* = 3**	2797 (A)	2819, 2818, 2817	terminal Al-(O-D) stretch
	2714 (B)	2746, 2742, 2742	bridging Al_2-(μ_2-O-D) stretch
	944 (E)	979, 949, 949	Al-OD stretch
	715 (F), 650 (G)	727, 727, 667, 666, 648, 648	Al_2-(μ_2-OD) in-plane bend
	650 (G)	658, 649	Al_3-(μ_3-O) stretch
***n* = 4**	2807 (A), 2750 (C)	2818, 2817, 2816, 2788[d]	terminal Al-(O-D) stretch
	2750 (C), 2688 (B), 2352 (D)	2759, 2717, 2715, 2359[d]	bridging Al_2-(μ_2-O-D) stretch
	942 (E), 743 (G)	965, 942, 929, 739[d]	Al-OD stretch
	790 (F), 698 (H), 653 (I)	852[d], 794, 768, 702, 670	Al_2-(μ_2-O-D) in-plane bend
	613 (J), 578 (K), 523 (L)	670, 648, 608, 570, 523	Al_2-(μ_2-O-D) stretch

[a] $[Al_3O_4]^+ (He)_3$. [b] $[Al_3O_4 (D_2O)]^+ D_2$. [c] Al_3-(μ_3-O) in planar bicyclic structure. [d] hydrogen-bonded.

Table S2 Calculated unscaled and scaled wavenumbers in cm^{-1} of O-D stretch modes of $[Al_3O_4(D_2O)_n]^+$ together with IR intensities in km/mol and O-D bond distances in pm using B3LYP/TZVPP. The coordination numbers (CN) refer to the Al-Atoms to which the OD groups are bonded. The scaling factor is 0.9732 and is calculated as the ratio between the averages of experimental and computational OD symmetric and antisymmetric stretching frequencies of D_2O.

System			CN		Exp	DFT		DFT scaled	Dev	Intensity	Distance
					O-D	O-D	O-H	O-D			O-D
D_2O (ν_{as})					2788	2865.97	3910.12	2789.06	1.1	28.7	96.1
D_2O(ν_s)					2672	2744.59	3807.32	2670.94	-1.1	3.6	96.1
½(ν_{as} + ν_s)					2730	2805.28	3858.72	2730.00			
***n* = 1**	**(C_{2v})**	μ_1	III		2806 (A)	2875.50	3942.27	2798.34	-7.7	60.2	95.6
		μ_1	III		2806 (A)	2874.15	3940.79	2797.02	-9.0	269.3	95.6
***n* = 2**	**(C_S)**	μ_1	III		2800 (A)	2878.27	3947.79	2801.03	1.0	117.1	95.5
		μ_1	III		2800 (A)	2870.20	3935.69	2793.18	-6.8	77.6	95.6
		μ_1	III		2800 (A)	2868.38	3933.44	2791.41	-8.6	237.5	95.7
		μ_2	III	III	2651 (B)	2732.78	3754.61	2659.45	8.5	113.3	96.9
***n* = 3**	**(C_3)**	μ_1	IV		2797 (A)	2896.85	3971.23	2819.11	22.1	68.6	95.4
		μ_1	IV		2797 (A)	2995.31	3969.70	2817.61	20.6	168.0	95.4
		μ_1	IV		2797 (A)	2895.09	3969.43	2817.40	20.4	169.8	95.4
		μ_2	IV	IV	2714 (B)	2821.76	3871.50	2746.04	32.0	118.6	96.0
		μ_2	IV	IV	2714 (B)	2817.87	3867.55	2742.25	28.3	127.8	96.0
		μ_2	IV	IV	2714 (B)	2817.71	3867.33	2742.10	28.1	127.7	96.0
***n* = 4**	**(C_S)**	μ_1	IV		2807 (A)	2896.03	3970.53	2818.31	11.3	83.6	95.4
		μ_1	IV		2807 (A)	2894.62	3969.04	2816.94	9.9	105.8	95.4
		μ_1	IV		2807 (A)	2893.78	3968.79	2816.13	9.1	195.0	95.4
		μ_1	IV		2750 (C)	2864.61	3931.11	2787.74	37.7	87.6	95.6
		μ_2	IV	IV	2750 (C)	2835.45	3890.61	2759.36	9.3	131.9	95.9
		μ_2	IV	IV	2688 (B)	2791.97	3834.07	2717.05	29.1	85.8	96.3
		μ_2	IV	IV	2688 (B)	2789.57	3832.07	2714.71	26.7	133.1	96.3
		μ_2	IV	IV	2352 (D)	2423.62	3323.81	2358.58	6.6	426.5	99.0

S4. Characteristic IR absorption regions

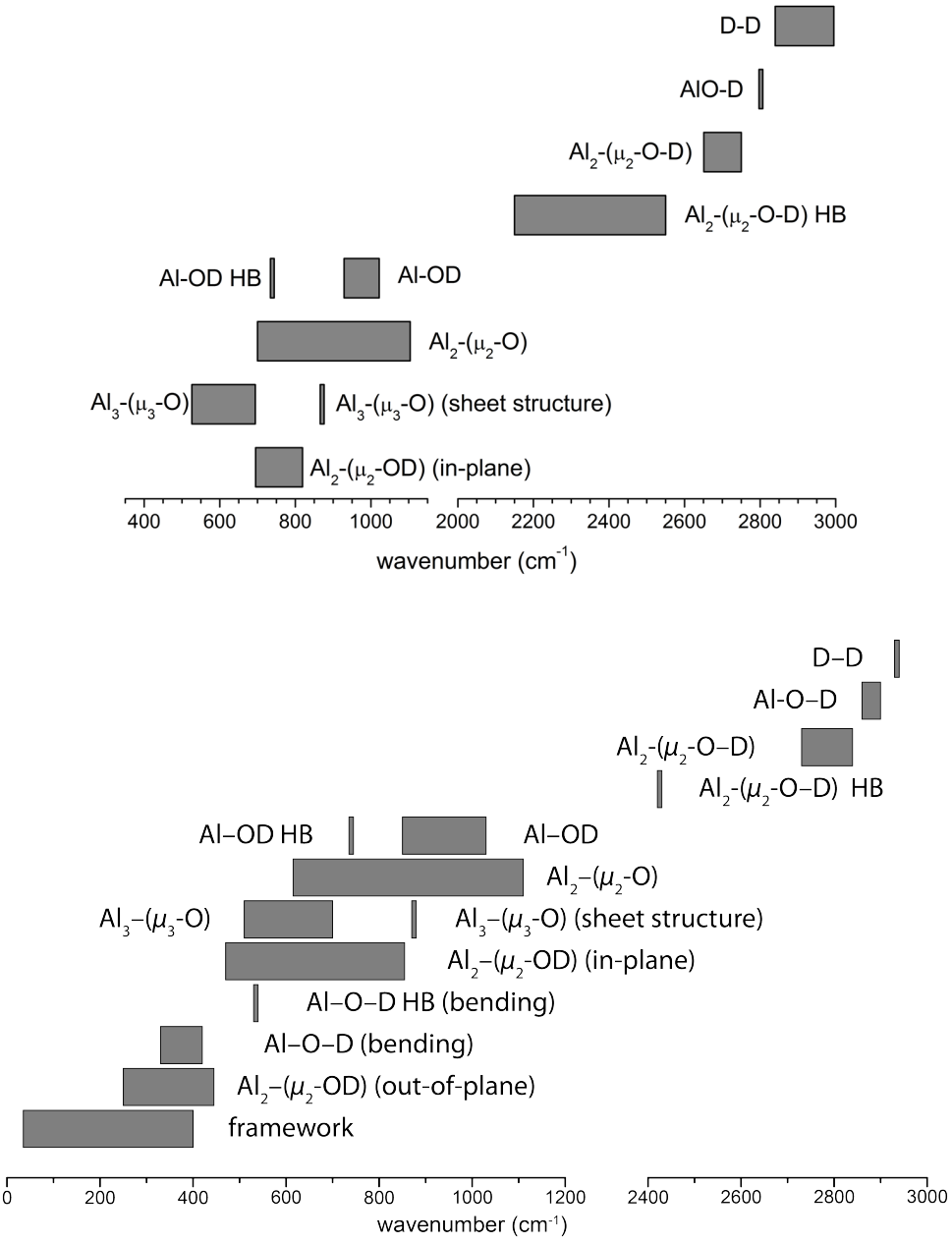

Figure S10 Characteristic IR absorption regions, determined from experimental (top) and calculated (bottom) gas phase vibrational spectra of $[Al_3O_4\ (D_2O)_{0\text{-}4}]^+$.

Four characteristic absorption regions are identified in the fingerprint spectral region. Al-OD stretching modes involving terminal hydroxyl groups are found at highest energy (1030 –

850 cm^{-1}), followed by Al_2-(μ_2-O) stretching modes involving bridging O atoms (1100 – 615 cm^{-1}). Al_3-(μ_3-O) stretching modes (700 – 510 cm^{-1}) absorb at lower energies. Al_2-(μ_2-OD) in-plane bending modes are found in the 855 – 470 cm^{-1} region.

The O-D stretching region extends roughly from 2810 cm^{-1} down to 2650 cm^{-1} and can be grouped into two non-overlapping regions, see Figure S8. The terminal O-D stretches are found in the narrow region between 2810 and 2790 cm^{-1}. The bridging μ_2-O-D stretches lie well separated between 2750 and 2650 cm^{-1}. Hydrogen-bonded O-D stretches are found even further to red, below 2400 cm^{-1}.

S5. Total energies

Table S3 Absolut electronic energy values and corresponding zero point vibration energies (Hartree) of all $[Al_3O_4\ (D_2O)_n]^+$ isomers shown in Figures S2-S7,of D_2O, D_2 and the He atom calculated with B3LYP/TZVPP.

System	Isomer [c]			
	1	**2**	**3**	**4**
***n* = 0**	-1036.8785958[a]	-1028.1465494	-1028.0744856	
	0.0231449	0.0196200	0.0178175	
***n* = 1**	-1105.9294880[b]	-1104.7437237	-1104.7426153	-1104.6700521
	0.0467375	0.0364389	0.0363021	0.0385932
***n* = 2**	-1181.2797148	-1181.2678900	-1181.2538987	
	0.0552406	0.0554691	0.0555226	
***n* = 3**	-1257.8217400	-1257.7987099	-1257.7695386	
	0.0743186	0.0738021	0.0748833	
***n* = 4**	-1334.2944410	-1334.2898490	-1334.2861279	
	0.0926036	0.0925712	0.0935262	
***n* = 5**	-1410.7597297	-1410.7548531	-1410.7534269	
	0.1125109	0.1116041	0.1107910	
D_2O	-76.4295903			
	0.0155042			
D_2	-1.1732476			
	0.0071153			
He	-2.9059107			

[a] $[Al_3O_4]^+(He)_3$. [b] $[Al_3O_4(D_2O)]^+D_2$. [c] see Figs. S4 – S9 for isomer numbers.

S6. Cartesian atomic coordinates (in Bohr) of global energy minimum structures

System	Atom	x	y	z
***n*=0**	Al	-0.6351	-0.5495	0.2322
	Al	-2.0611	0.6115	-1.3549
	Al	0.3518	0.8569	-1.4853
	O	0.8148	0.3917	0.1178
	O	-2.2489	0.0783	0.2828
	O	-0.9955	1.8646	-1.8987
	O	-0.7257	-0.6279	-1.6025
***n*=1**	Al	1.7722	-0.0012	0.0090
	Al	-1.7722	0.0005	-0.0075
	Al	0.0008	1.7713	0.0105
	O	2.8547	-1.2362	0.0044
	O	-0.0001	-0.1438	0.0006
	O	1.6862	1.7389	0.0183
	O	-1.6845	1.7404	0.0020
	O	-2.8561	-1.2333	-0.0195
	H	3.8075	-1.3187	0.0081
	H	-3.8086	-1.3178	-0.0260
***n*=2**	Al	2.0390	-0.0431	0.0002
	Al	-0.5408	1.6853	-0.0065
	Al	-0.6637	-1.5618	0.0116
	O	1.0893	1.3792	-0.0092
	O	0.9891	-1.3993	0.0146
	O	3.6968	-0.0085	-0.0074
	O	-1.4295	0.0927	0.0023
	O	-1.8894	-2.6708	0.0109
	O	-1.6757	2.8861	-0.0130
	H	-1.9295	-3.6264	0.0147
	H	4.3533	-0.7027	-0.0028
	H	-2.3978	0.1273	0.0007
	H	-1.6410	3.8420	-0.0159
***n*=3**	Al	1.5639	-0.0391	-0.1364
	Al	-0.8158	-1.3356	-0.1296
	Al	-0.7487	1.3733	-0.1317
	O	0.8159	-1.4919	0.6979
	O	-1.6949	0.0411	0.7059
	O	-1.4070	2.8506	-0.4814
	O	0.8867	1.4512	0.6956
	O	-0.0025	-0.0013	-1.0513
	O	3.1713	-0.2115	-0.4900
	O	-1.7714	-2.6409	-0.4784
	H	1.2940	2.1374	1.2300
	H	1.2078	-2.1850	1.2348
	H	3.8464	0.2563	-0.9748

	H	-2.4899	0.0506	1.2445
	H	-2.1479	3.2023	-0.9681
	H	-1.7077	-3.4575	-0.9671
***n*=4**	Al	1.0669	-1.3861	0.0429
	Al	1.1452	1.3232	0.0489
	Al	-1.7760	0.0516	-0.0022
	O	0.9629	-0.0245	-1.1698
	O	1.8505	2.8197	-0.0344
	O	1.6880	-2.9192	-0.0473
	O	-0.5983	1.3992	0.5199
	O	1.8119	-0.0541	1.0565
	O	-0.6783	-1.3648	0.5123
	O	-3.1499	0.0711	0.9522
	O	-1.5844	0.0630	-1.7164
	H	-0.9611	2.1588	0.9879
	H	0.1814	0.0006	-1.7764
	H	2.6860	3.1907	-0.3063
	H	2.2735	-0.0702	1.8970
	H	2.5009	-3.3335	-0.3252
	H	-1.0857	-2.1024	0.9789
	H	-4.0867	0.1385	0.7868
	H	-2.2469	0.0386	-2.4054
***n*=5**	Al	-0.3336	1.9763	-0.1239
	Al	-1.4024	-0.6025	0.2230
	Al	1.7903	-0.4475	0.1780
	O	-2.7839	-1.3810	0.7975
	O	0.2496	-0.9941	1.0010
	O	-1.3653	1.1574	1.0912
	O	-0.2764	3.6066	-0.4550
	O	3.2015	-0.4779	1.0868
	O	1.3631	1.3559	0.0829
	O	-0.9555	0.6071	-1.1299
	O	-1.0493	-1.9816	-1.1091
	O	1.4849	-1.2415	-1.3417
	H	-3.5308	-1.0553	1.2939
	H	3.8965	-1.1229	1.1927
	H	2.0807	1.9773	0.2496
	H	0.2763	-1.1285	1.9529
	H	-1.6632	1.4201	1.9618
	H	-0.9217	4.2938	-0.6016
	H	2.1465	-1.4006	-2.0160
	H	-0.6748	0.3303	-2.0049
	H	-1.4454	-2.8517	-0.9869
	H	-0.0872	-2.0397	-1.3424